Theory of spin transport induced by ferromagnetic proximity on a two-dimensional electron gas

J. P. McGuire, C. Ciuti, and L. J. Sham
Department of Physics, University of California—San Diego, La Jolla, California 92093-0319, USA
(Received 15 September 2003; revised manuscript received 15 January 2004; published 30 March 2004)

A theory of the proximity effects of the exchange splitting in a ferromagnetic metal on a two-dimensional electron gas (2DEG) in a semiconductor is presented. The resulting spin-dependent energy and lifetime in the 2DEG create a marked spin splitting in the driven in-plane current. The theory of the planar transport allows for current leakage into the ferromagnetic layer through the interface, which leads to a competition between drift and diffusion. The spin-dependent in-plane conductivity of the 2DEG may be exploited to provide the possibility for spintronics devices based on planar devices in a field-effect transistor configuration. An illustrative example is provided through the transport theory of a proposed spin valve which consists of a field-effect transistor configuration with two ferromagnetic gates. Results are provided for two experimentally accessible systems: the silicon inversion layer and the naturally formed InAs accumulation layer.

DOI: 10.1103/PhysRevB.69.115339 PACS number(s): 85.75.−d, 72.25.−b, 73.43.Qt, 73.20.−r

I. INTRODUCTION

The emerging field of spintronics aims to implement semiconductor devices which utilize both the carrier charge and spin degrees of freedom.[1] Research in the field has been inspired by the early device proposal of Datta and Das,[2] which consists of spin injection through a ferromagnetic-semiconductor interface and spin manipulation using the Rashba spin-orbit effect.[3] There has been recent progress in achieving maximum spin injection[4–7] and in characterization of the Rashba effect.[8–11] However, a spin device based on injection has a high tunnel resistance, analogous to a Schottky diode. We have suggested an alternate approach of spin creation and manipulation which makes use of the proximity effects of a ferromagnet on a semiconductor.[12] The eventual device would avoid the high tunneling resistance by keeping the main driven current path entirely in the semiconductor through normal ohmic nonmagnetic leads, resembling the field-effect transistor design.

In this paper we present a comprehensive theory of the consequences of the ferromagnetic proximity on the equilibrium and transport properties of the electrons in the semiconductor. First, we fully examine the coupling of a semiconductor two-dimensional electron gas (2DEG) with a ferromagnetic layer through a very thin potential barrier. Explicit calculations are provided for two realizable systems, the silicon inversion layer and the naturally formed InAs surface layer, both with ferromagnetic gates. The coupling is conveniently treated by a Green's function method which can account for realistic confinement for the semiconductor 2DEG as well as the effects of a short electron mean free path in the ferromagnet. The complex self-energy of the 2DEG due to the interaction with the ferromagnet contains both static and dynamic effects (a Zeeman-like splitting and spin-dependent scattering times, respectively). Both properties alter the in-plane conductivity and can be exploited through the spin-dependent transport under the ferromagnetic gate. As an illustration of the possible consequences of the ferromagnetic proximity on the semiconductor, we show in detail the behavior of the density and current in a previously proposed[12] planar spin valve in MOSFET-style configuration with two adjacent ferromagnetic gates with reversible magnetizations, where MOSFET stands for metal-oxide-semiconductor field-effect transistor. We find that the proposed device has a significant magnetoresistance effect for reasonable system parameters.

The coupling of the 2DEG to the ferromagnetic gate exponentially decreases with their separation by a potential barrier. Our study includes oxide barriers down to the smallest state-of-the-art thickness and direct contact between the 2DEG and the ferromagnet to ensure sizable spin effects. A consequence of this requirement for ultrathin oxides is that current leakage into the ferromagnetic gate(s) becomes an integral part of the in-plane electron transport. This naturally results in the need to consider both the current driven by the in-plane electric field and the diffusion driven by the density gradient, analogous to the bulk case.[13,14] Although such leakage effects would decrease the efficiency of normal field-effect transistors, we find that they actually enhance the spin dependence of the electron transport from the source to the drain.

We argue that the relevance of proximity effects between a semiconductor and a ferromagnet is supported by recent experiments. A series of optical Faraday rotation experiments[15,16] have shown that unpolarized nonequilibrium electrons in a semiconductor can spontaneously acquire a net spin polarization in the presence of a ferromagnetic interface. We have interpreted[18] the observed effect as arising from the spin-dependent reflection of electrons off the ferromagnetic interface. Assuming negligible spin scattering at the interface, the spontaneous spin polarization produced in the semiconductor is indicative of the strength of the coupling across the semiconductor-ferromagnet junction. In addition, replacing the Schottky barrier[15–17] with a much thinner oxide will only increase the interaction.

Proximity effects between dissimilar materials have been used to describe how the ordered state of one medium induces a similar order in the other medium which is otherwise normal. The induced order parameter decays away from the interface. The common examples are the proximity effects between a superconductor and a normal metal (or a semiconductor 2DEG) and between a ferromagnet and a paramag-

netic metal. The induced ferromagnetic order in a nonmagnetic metal is weak and requires the metal to be superparamagnetic,[19] such as Pd or Pt. In this paper we concentrate on the proximity effect between a ferromagnet and a semiconductor 2DEG. The 2DEG is examined rather than the bulk semiconductor because it has two advantages: (1) the 2DEG is confined near the interface where it is more susceptible to the influence of the exchange-split electrons in the ferromagnet, and (2) while the induced polarization in the 2DEG may be too small for a magnetization measurement, the influence on the spin-polarized transport is the ultimate goal. Moreover, there exists a large amount of knowledge and technology dedicated to the manipulation of semiconductor 2DEG's, further increasing the potential for spintronics devices.

In Sec. II we explain the model of the semiconductor 2DEG ferromagnet used in the calculations, followed by the derivation of an effective tight-binding Hamiltonian (Sec. II A) which is used in a Green's function formalism (Sec. II B) to approximate the coupling between the semiconductor 2DEG and the ferromagnet. In Sec. III we calculate the self-energy of the 2DEG coupled to the ferromagnet for two experimentally realizable systems, the silicon inversion layer (Sec. III A) and the naturally-formed InAs surface layer (Sec. III B). In Sec. IV we derive the equations and show representative results for the 2DEG density and in-plane current for the silicon inversion layer (Sec. IV A) and for the InAs surface layer (Sec. IV B). In Sec. V we calculate the 2DEG density and current for a spin-valve with two ferromagnetic gates for the silicon (Sec. V A) and the InAs (Sec. V B) systems. We summarize our findings and draw conclusions in Sec. VI.

II. MODEL OF THE ELECTRONIC STRUCTURE

The two particular systems we will consider have band diagrams as shown in Fig. 1. The semiconductor 2DEG is on the right, which is induced by a gate bias for the silicon inversion layer [Fig. 1(a)] and is naturally formed for the InAs surface layer [Fig. 1(b)]. The left side is the ferromagnet, which is modeled as parabolic bands split by the exchange energy Δ.[20] A very thin oxide separates the 2DEG from the ferromagnet. This oxide is necessary in the silicon system because a gate bias is necessary for the creation of the inversion layer. Because the surface layer in the InAs system forms naturally, no gate bias is necessary and hence intimate contact (no oxide barrier) is possible between the InAs surface layer and the ferromagnet.

All calculations are done within the effective-mass approximation in a one-dimensional model of the interface (the in-plane wave vector is not conserved across the interface[21,22]). These, along with the exchange-split parabolic band approximation, cannot possibly account for all band effects in the ferromagnet. We wish to show in a transparent way how the spin dependence in the ferromagnet can influence the 2DEG; more realistic calculations will be necessary for comparison with experiment, but the essential effects we deduce here should remain valid. In particular, the one-dimensional parabolic bands we use here must be replaced

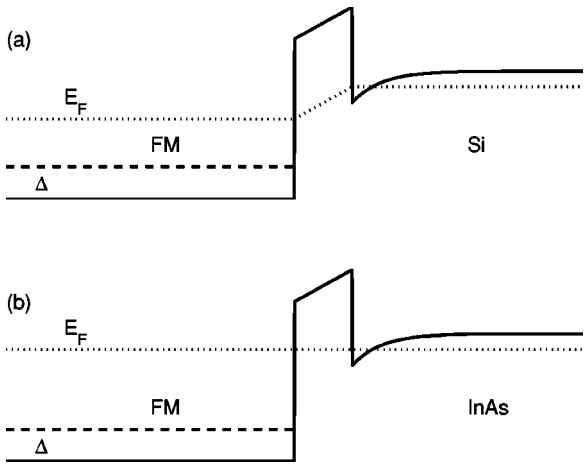

FIG. 1. Band diagrams for (a) the silicon inversion layer and (b) the InAs surface layer, both separated from a ferromagnet by a thin oxide barrier. The ferromagnet, with exchange splitting Δ, is on the left and the semiconductor 2DEG is on the right. In (a), the Fermi level in the ferromagnet is lower than the Fermi level in the silicon inversion layer. In (b), the Fermi level in the ferromagnet is equal to the Fermi level in the InAs surface layer.

with the realistic three-dimensional band structure; the spin dependence in the one-dimensional model due to the exchange splitting of the parabolic bands only mimics the real spin dependence in the ferromagnet.

The two spin channels are considered to be completely decoupled and are labeled by $+$ and $-$. Experimentally, it appears that the spin lifetime in semiconductor heterostructures can persist for long times and over long distances, including through heterostructure interfaces.[23–26] We neglect any mixing due to the spin-orbit effect or other spin-flip processes. The neglect of the Rashba spin-orbit interaction[3] is valid in Si and holds less well in the InAs surface layer, but sufficiently well without gate voltage.[9] Coupling of the two spin channels decreases the magnitude of the spin effects presented here.

In a recent article[12] we reported the calculation of the coupling between a silicon inversion layer and a ferromagnetic gate in the effective-mass approximation using a triangular potential in the semiconductor region. The simplicity of the potential allowed us to use the wave function matching conditions to derive an equation specifying the complex energy of the eigenstate of the coupled system. Strong scattering in the ferromagnet was incorporated by putting a phenomenological damping into the wave function in the ferromagnet region. The triangular potential approximation, although valid in the silicon system for strong inversion,[27] is not appropriate for the weakly confined 2DEG at the InAs surface. For this reason, the InAs potential is calculated self-consistently with the surface layer density distribution using the coupled Schrodinger and Poisson equations. A Green's function method is developed to calculate the coupling between the semiconductor 2DEG and the ferromagnet which works for both the triangle potential in the silicon system and the self-consistent potential in the InAs system. In addition, the Green's function approach is ideal because it allows us to include scattering in a more natural and rigorous manner

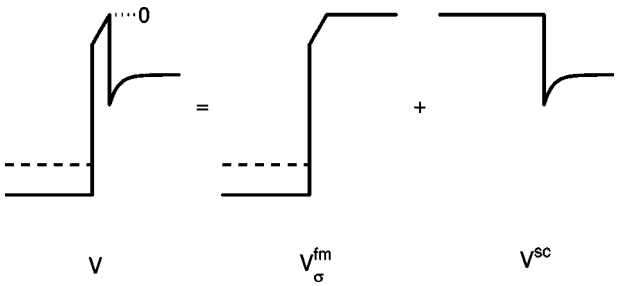

FIG. 2. A cartoon of the splitting up of the potential. The original band diagram is on the left, and this is split into a *ferromagnetic* potential $V_\sigma^{\rm fm}$ and a *semiconductor* potential $V^{\rm sc}$.

than in the wave-function approach. In brief, the coupled semiconductor 2DEG-ferromagnet system is solved in three steps: (1) Separate the semiconductor and ferromagnet regions and solve them separately; (2) approximate the coupling between the two subsystems by transforming the original effective-mass Hamiltonian into a ''tight-binding'' (i.e., tunneling) Hamiltonian; (3) calculate the self-energy of 2DEG electrons due to the interaction with the ferromagnet.

A. Derivation of the effective Hamiltonian

The effective-mass Hamiltonian for the ferromagnet-oxide-semiconductor junction (see Fig. 1),

$$H=\frac{-\hbar^2}{2}\frac{d}{dz}\left(\frac{1}{m^\star(z)}\frac{d}{dz}\right)+\left(U_{\rm fm}+\frac{\Delta}{2}\boldsymbol{\sigma}\cdot\hat{\mathbf{M}}\right)\Theta(-z)+U_{\rm b}(z)\Theta(z_{\rm b}-z)\Theta(z)+U_{\rm sc}(z)\Theta(z-z_{\rm b}), \quad (1)$$

can be written as $H=K+V^{\rm sc}+V_\sigma^{\rm fm}$, where K is the kinetic energy and the *semiconductor* and *ferromagnet* potentials are defined, respectively, as

$$V^{\rm sc}(z)=U_{\rm sc}(z)\Theta(z-z_{\rm b})+0\Theta(z_{\rm b}-z),$$

$$V_\sigma^{\rm fm}(z)=U_{\rm b}(z)\Theta(z_{\rm b}-z)\Theta(z)+0\Theta(z-z_{\rm b})+\left(U_{\rm fm}+\frac{\Delta}{2}\boldsymbol{\sigma}\cdot\hat{\mathbf{M}}\right)\Theta(-z). \quad (2)$$

The zero of energy is put at the right side of the barrier for convenience. Basically, $V_\sigma^{\rm fm}(z)$ consists of the spin-dependent ferromagnet potential ($U_{\rm fm}+\Delta\boldsymbol{\sigma}\cdot\hat{\mathbf{M}}/2$) for $z<0$, the oxide barrier potential $U_{\rm b}(z)$ for $0<z<z_{\rm b}$, and is zero for $z>z_{\rm b}$. From now on we choose the spin-quantization axis to be parallel to the magnetization $\mathbf{M}$ in the ferromagnet, so that $V_\sigma^{\rm fm}\to V_\pm^{\rm fm}$. The semiconductor potential $V^{\rm sc}(z)$ consists of the 2DEG confinement potential $U_{\rm sc}(z)$ for $z>z_{\rm b}$ and is zero everywhere else.

This separation of the potential (illustrated in Fig. 2) is convenient because it allows us to solve the two subsystems with potentials $V_\pm^{\rm fm}(z)$ and $V^{\rm sc}(z)$ separately, and then calculate the coupling between them. The subsystems are solved, yielding the semiconductor eigenstates $\{\chi_n^{\rm sc}(z)\}$ with energy $\epsilon_n^{\rm sc}$ and the ferromagnet eigenstates $\{\chi_{k,\pm}^{\rm fm}(z)\}$ with energy $\epsilon_{k,\pm}^{\rm fm}$. The finite overlap between the wave functions for the two subsystems implies that they are not mutually orthogonal. To ensure proper Fermionic anticommutation relations between the operators in all parts of the system, we orthogonalize the ferromagnetic eigenstates to the discrete 2DEG eigenstates,

$$\phi_{k,\pm}^{\rm fm}(z)=\chi_{k,\pm}^{\rm fm}(z)-\sum_n \chi_n^{\rm sc}(z)\langle\chi_n^{\rm sc}|\chi_{k,\pm}^{\rm fm}\rangle. \quad (3)$$

This allows us to write a general state of the system as

$$\psi_\pm(z)=\sum_n \chi_n^{\rm sc}(z)a_{n,\pm}+\sum_k \phi_{k,\pm}^{\rm fm}(z)c_{k,\pm}, \quad (4)$$

where $a_{n,\pm}$ and $c_{k,\pm}$ are the Fermion operators for the 2DEG state $\chi_n^{\rm sc}(z)$ and the orthogonalized ferromagnet state $\phi_{k,\pm}^{\rm fm}(z)$, respectively. The only Fermion operators that do not anticommute properly are

$$\{c_{k,\pm},c_{k',\pm}^\dagger\}=\delta_{k,k'}-2\langle\chi_n^{\rm sc}|\chi_{k,\pm}^{\rm fm}\rangle\langle\chi_{k',\pm}^{\rm fm}|\chi_n^{\rm sc}\rangle\approx\delta_{k,k'}. \quad (5)$$

As an approximation we keep only terms that have a single exponentially decaying term in an overlap integral. Since $\langle\chi_n^{\rm sc}|\chi_{k,\pm}^{\rm fm}\rangle\langle\chi_{k',\pm}^{\rm fm}|\chi_n^{\rm sc}\rangle$ contains the product of two overlap integrals with an exponentially decaying term, we neglect it leaving an approximate set of Fermionic operators.

Now we must calculate all the matrix elements involved in $\langle\psi_\pm|K+V_\pm^{\rm fm}+V^{\rm sc}|\psi_\pm\rangle$, keeping the approximation as mentioned above. The matrix elements between different semiconductor states are

$$\langle\chi_{n'}^{\rm sc}|K+V_\pm^{\rm fm}+V^{\rm sc}|\chi_n^{\rm sc}\rangle=\epsilon_n^{\rm sc}\delta_{n,n'}+V_{n',n,\pm}^{\rm fm}\approx\epsilon_n^{\rm sc}\delta_{n,n'}, \quad (6)$$

where

$$V_{n',n,\pm}^{\rm fm}=\int dz(\chi_{n'}^{\rm sc})^\star V_\pm^{\rm fm}\chi_n^{\rm sc} \quad (7)$$

is neglected because the integral contains two exponentially decaying functions. The matrix elements between a semiconductor state and a ferromagnet state are

$$\langle\phi_{k,\pm}^{\rm fm}|K+V_\pm^{\rm fm}+V^{\rm sc}|\chi_{n,\pm}^{\rm sc}\rangle=\epsilon_n^{\rm sc}\langle\phi_{k,\pm}^{\rm fm}|\chi_n^{\rm sc}\rangle+V_{k,n,\pm}^{\rm fm}=V_{k,n,\pm}^{\rm fm}, \quad (8)$$

where $\langle\phi_{k,\pm}^{\rm fm}|\chi_n^{\rm sc}\rangle=0$ because of the orthogonality between the semiconductor and ferromagnet states and

$$V_{k,n,\pm}^{\rm fm}=\int dz(\phi_{k,\pm}^{\rm fm})^\star V_\pm^{\rm fm}\chi_n^{\rm sc} \quad (9)$$

is kept because there is only a single exponentially decaying wave function in the nonzero integration region. Finally, the matrix elements between ferromagnetic states are

$$\langle\phi_{k,\pm}^{\rm fm}|K+V_\pm^{\rm fm}+V^{\rm sc}|\phi_{k',\pm}^{\rm fm}\rangle=\epsilon_{k,\pm}^{\rm fm}\delta_{k,k'}+W_{k,k',\pm}\approx\epsilon_{k,\pm}^{\rm fm}\delta_{k,k'}, \quad (10)$$

where $\epsilon_{k,\pm}^{\rm fm}$ is the energy of the state $\chi_{k,\pm}^{\rm fm}$ before the orthogonalization to the 2DEG states and

$$W_{k,k',\pm}=\langle\chi^{\rm fm}_{k',\pm}|V^{\rm sc}|\chi^{\rm fm}_{k,\pm}\rangle+\sum_n\,[(\epsilon^{\rm sc}_n\langle\chi^{\rm fm}_{k',\pm}|\chi^{\rm sc}_n\rangle+V^{\rm fm}_{k',n,\pm})\times\langle\chi^{\rm sc}_n|\chi^{\rm fm}_{k,\pm}\rangle+(\epsilon^{\rm sc}_n\langle\chi^{\rm sc}_n|\chi^{\rm fm}_{k,\pm}\rangle+V^{\rm fm}_{n,k,\pm})\times\langle\chi^{\rm fm}_{k',\pm}|\chi^{\rm sc}_n\rangle] \tag{11}$$

is neglected because all terms contain more than a single exponentially decaying function.

We are left with an effective Hamiltonian with a simple tight-binding form:

$$H=\sum_{n,\sigma}\,a^\dagger_{n,\sigma}\epsilon^{\rm sc}_n a_{n,\sigma}+\sum_{k,\sigma}\,c^\dagger_{k,\sigma}\epsilon^{\rm fm}_{k,\sigma}c_{k,\sigma}+\sum_{n,k,\sigma}\,(a^\dagger_{n,\sigma}V^{\rm fm}_{n,k,\sigma}c_{k,\sigma}+c^\dagger_{k,\sigma}V^{\rm fm}_{k,n,\sigma}a_{n,\sigma}). \tag{12}$$

This Hamiltonian represents the coupling between the quantum confined electrons in the semiconductor and the broad spin-dependent continuum in the ferromagnet. We solve the Hamiltonian below using a Green's function approach.

B. Green's functions for the coupled system

We are interested in the properties of the 2DEG electrons due to the coupling with the ferromagnet. The retarded Green's functions relevant to our calculations are

$$G_{n,\pm}(t)=-i\Theta(t)\langle\{a_{n,\pm}(t),a^\dagger_{n,\pm}(0)\}\rangle, \tag{13}$$

$$G_{k,\pm}(t)=-i\Theta(t)\langle\{c_{k,\pm}(t),c^\dagger_{k,\pm}(0)\}\rangle, \tag{14}$$

$$G_{k,n,\pm}(t)=-i\Theta(t)\langle\{c_{k,\pm}(t),a^\dagger_{n,\pm}(0)\}\rangle, \tag{15}$$

where $\Theta(t)$ ensures us that $t>0$. The unperturbed Green's functions when the coupling $V^{\rm fm}_{n,k,\pm}$ is zero are

$$G^{(0)}_{n,\pm}(E)=(E-\epsilon^{\rm sc}_n+i0^+)^{-1}, \tag{16}$$

$$G^{(0)}_{k,\pm}(E)=(E-\epsilon^{\rm fm}_{k,\pm}+i\gamma^{\rm fm}_{k,\pm})^{-1}. \tag{17}$$

Note that the ferromagnet is assumed to be a dirty conductor, so that an imaginary part has been added to the ferromagnet energy to account for strong spin-dependent scattering in the ferromagnet:[28] $\epsilon^{\rm fm}_{k,\pm}\rightarrow\epsilon^{\rm fm}_{k,\pm}-i\gamma^{\rm fm}_{k,\pm}$.

Calculating the Green's functions with the interaction from the Hamiltonian and Fourier transforming, we have the following equation for the full 2DEG Green's function:

$$G_{n,\pm}(E)=[E-\epsilon^{\rm sc}_n+i0^+-\Sigma_{n,\pm}(E)]^{-1}, \tag{18}$$

where the self-energy of the 2DEG electrons is

$$\Sigma_{n,\pm}(E)=\sum_k\,V^{\rm fm}_{n,k,\pm}G^{(0)}_{k,\pm}(E)V^{\rm fm}_{k,n,\pm}. \tag{19}$$

The effect of the coupling on the 2DEG eigenstates is found from the complex energy $\tilde{E}$ which satisfies

$$\tilde{E}-\epsilon^{\rm sc}_n+i0^+-\Sigma_{n,\pm}(\tilde{E})=0. \tag{20}$$

The real part of the 2DEG self-energy, $\Delta_{n,\pm}(\tilde{E})={\rm Re}[\Sigma_{n,\pm}(\tilde{E})]$, is the spin-dependent level shift of the 2DEG subbands due to the coupling with the ferromagnet. This gives the 2DEG a static spin splitting, which is $|\Delta_+-\Delta_-|$ if only one 2DEG subband is occupied. The two spin channels will have different densities, $N_+\neq N_-$. The imaginary part of the 2DEG self-energy, $\hbar/2\tau_{n,\pm}(\tilde{E})=-{\rm Im}[\Sigma_{n,\pm}(\tilde{E})]$, is related to the lifetime of the 2DEG electrons to scatter in a spin-dependent way off the ferromagnet. This new spin-dependent scattering channel will result in different conductivities for the two spin channels, and will be addressed in Sec. IV.

III. RESULTS FOR RELEVANT SYSTEMS

We have shown how to calculate the spin-dependent effects for the coupled 2DEG-ferromagnet system. In this section we apply this method to two experimentally realizable systems: the silicon inversion layer and the naturally formed InAs surface layer. Silicon MOSFET-type devices are ubiquitous in present technology, and any spintronics device in this system would have a strong industrial base. The inversion layer is created by a gate bias, which increases the coupling with the ferromagnet by pressing the electrons close to the interface with the (ferromagnetic) gate. The need for ultrathin oxide barriers (to increase the coupling) implies that 2DEG electrons can irreversibly tunnel into the ferromagnet. We shall account for the effects of the current leakage. Since the removal of the oxide barrier (provided that it is not replaced by a Schottky barrier) brings simplicity, we also examine the naturally occurring InAs accumulation layer which forms an ohmic contact with the metal. The 2DEG forms at the interface without the need for a gate bias, so the leakage of electrons is not a problem in this system. However, the confinement of electrons in such a surface layer is quite weak.

We start with calculation of the ferromagnet subsystem wave functions and energy eigenvalues; we will show below how to treat the semiconductor subsystem. The ferromagnet subsystem is made of the ferromagnet potential for $z<0$, the barrier potential for $0<z<z_{\rm b}$, and is zero for $z>z_{\rm b}$. All states are included in the calculation that decay exponentially for $z>z_{\rm b}$ (all states with energy less than zero). To fix the normalization of the ferromagnet states and the ferromagnet density of states, the ferromagnet continuum is approximated by a large but finite box (see Fig. 3). Convergence is checked for both the size of the box and the number of points in the box.

The ferromagnet has the same parameters for all calculations below. The exchange-split parabolic bands have an effective mass equal to the free-electron mass m_0. The majority wave vector is $k^{\rm fm}_+=1.1$ Å^{-1} and the minority wave vector is $k^{\rm fm}_-=0.42$ Å^{-1},[20] corresponding to a majority Fermi energy of $U_{\rm fm}=4.6$ eV and an exchange energy of $\Delta=3.9$ eV. The ferromagnet is assumed to be dirty, so that the scattering is significant. We account for this by putting by hand an imaginary part into the ferromagnet energy eigen-

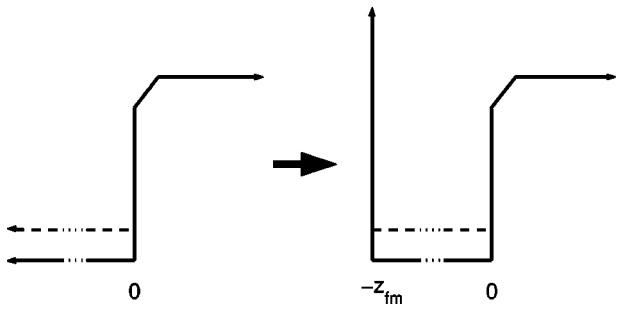

FIG. 3. The ferromagnet subsystem, approximated as a large but finite box. It consists of the exchange split ferromagnet potential, the barrier potential, and is zero for $z>z_b$. The wave function must vanish at the left boundary $z=-z_{fm}$.

values after calculating the particle-in-a-box eigenstates which is the same for all wave vectors, $\gamma_+^{fm}=1.1$ eV and $\gamma_-^{fm}=0.8$ eV.[28] We are left with the wave functions and complex energy eigenvalues for all states in the ferromagnet with the real part of their energy less than zero. Below we describe separately how we calculate the semiconductor subsystem for the two systems we consider in this paper.

A. Silicon inversion layer

The 2DEG in this system is strongly inverted at the interface and the triangular approximation to the semiconductor potential is adequate.[27] The dielectric constant in silicon is taken as $\epsilon_{Si}=11.7$, the longitudinal effective mass responsible for the confinement is $m^{\star}_{Si,l}=0.91m_0$, and the transverse effective mass relevant to the in-plane motion of the 2DEG is $m^{\star}_{Si,t}=0.19m_0$. The oxide barrier between the silicon and the ferromagnet is assumed to be SiO_2 with barrier height (from the ferromagnet Fermi level) $U_{SiO_2}=3.2$ eV, effective mass $m^{\star}_{SiO_2}=0.3m_0$, and dielectric constant $\epsilon_{SiO_2}=3.9$.[29] We assume that the electric field in the barrier, which is set by the bias between the silicon substrate and the ferromagnetic gate, is near its breakdown value of $E_{SiO_2}=12$ MV/cm. The electric field in the silicon responsible for the 2DEG confinement is then $E_{Si}=(\epsilon_{SiO_2}/\epsilon_{Si})E_{SiO_2}$. The density in the 2DEG is assumed to be 10^{12} cm^{-2}, corresponding to a Fermi energy of ≈ 6.3 meV.

The numerical results for the spin splitting $|\Delta_+-\Delta_-|$ (dotted line running from upper left to lower right) and the scattering times for the two spin channels τ_+ (full line running from lower left to upper right) and τ_- (dashed line running from lower left to upper right) are shown in Fig. 4 for $E_{SiO_2}=10$ MV/cm. The horizontal axis is the thickness of the oxide barrier; sizable coupling between the 2DEG and the ferromagnet occurs only for ultrathin oxides at the limit of current device fabrication techniques. The spin splitting is very small even for the thinnest oxide considered; at 6 Å barrier width, the spin-splitting of ≈ 0.1 meV versus the 2DEG Fermi energy of ≈ 6.3 meV yields a static spin polarization of the 2DEG $\approx 1\%$.

On the other hand, the scattering time for the two spin channels is a promising effect of the coupling that could be

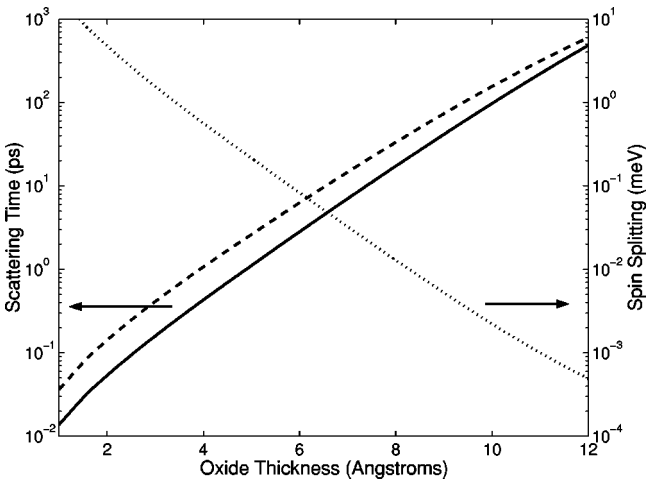

FIG. 4. A plot of the spin splitting $|\Delta_+-\Delta_-|$ (dotted line running from upper left to lower right) and the spin-dependent scattering times τ_+ (full line running from lower left to upper right) and τ_- (dashed line running from lower left to upper right) as a function of the thickness of the SiO_2 barrier for a silicon inversion layer. The parameters used are explained in the text.

used in a device. For 6 Å barrier width, the two spin channels have scattering times of ≈ 3 ps and 6 ps; the spin-dependent coupling to the ferromagnet has opened a new spin-dependent scattering channel for the 2DEG electrons. To utilize this effect in a device, the new scattering times must be comparable to the intrinsic scattering time for the silicon inversion layer (including phonons, impurities, defects, etc., but not including the effects of the nearby ferromagnetic layer), which at low temperatures is near 1 ps, corresponding to a mobility of $\approx$ 9000 cm^2/V s.[27] As is evident in the plot, the scattering times for the two spin channels approach this intrinsic value for very thin oxide thicknesses, while their relative ratio remains the same. Because the two times are near the intrinsic time, but are still quite different (more than a factor of 2), we would expect that any physical quantity that depends on the scattering time would see this spin effect. This will be addressed later when we discuss 2DEG transport under the gate.

B. InAs surface layer

The 2DEG at the InAs surface is naturally formed. As opposed to the strongly inverted silicon inversion layer discussed above, the confining potential in the InAs system is quite weak and a realistic calculation of the coupling requires that the potential be calculated self-consistently with the density distribution in the 2DEG. We use the coupled Schrödinger and Poisson equations in the semiconductor region $z>z_b$,

$$\frac{-\hbar^2}{2}\frac{\partial}{\partial z}\left(\frac{1}{m^{\star}}\frac{\partial \chi_n^{sc}}{\partial z}\right)+V^{sc}(z)\chi_n^{sc}(z)=\epsilon_n^{sc}\chi_n^{sc}(z), \quad (21)$$

$$\frac{\partial^2 V^{sc}}{\partial z^2}=\frac{-4\pi e^2}{\epsilon_{sc}}N_0\sum_n |\chi_n^{sc}(z)|^2, \quad (22)$$

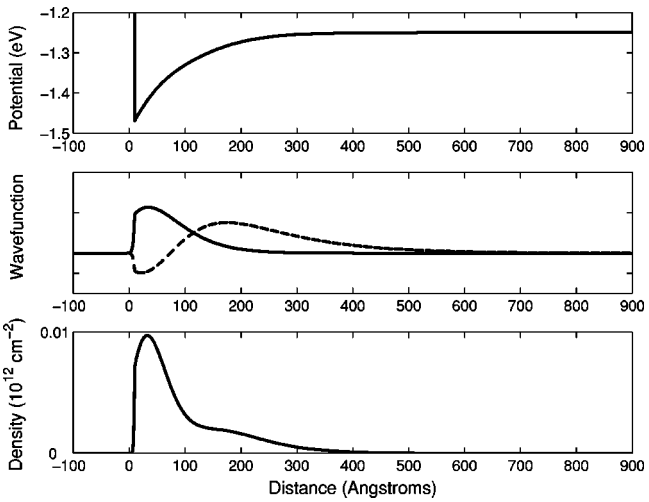

FIG. 5. (a) The calculated potential (eV) for the InAs surface layer with the parameters given in the text. The zero of energy is at the top right side of the barrier. (b) The wave functions for the two subbands (arbitrary units). (c) The density distribution in the 2DEG (arbitrary units).

where the total density in the 2DEG is kept fixed and $N_0=(2m^{\star}_{\mathrm{InAs}}/\pi\hbar^2)\Sigma_n(\epsilon_{\mathrm{F}}^{\mathrm{sc}}-\epsilon_n^{\mathrm{sc}})$. The band bending in the barrier is negligible. Unlike the silicon inversion layer, more than one subband in the InAs surface layer are occupied by electrons. Solving these equations simultaneously results in the 2DEG wave functions $\chi_n^{\mathrm{sc}}(z)$, energies ϵ_n^{sc}, and the semiconductor potential $V^{\mathrm{sc}}(z)$. The InAs parameters used in the calculation are an effective mass of $m^{\star}_{\mathrm{InAs}}=0.023m_0$, dielectric constant $\epsilon_{\mathrm{InAs}}=14.6$, and 2DEG density $N_0=10^{12}$ cm^{-2}. The barrier is taken as Al_2O_3 with a barrier height from the ferromagnet Fermi level of $U_{\mathrm{Al_2O_3}}=1.2$ eV, effective mass[30] $m^{\star}_{\mathrm{Al_2O_3}}=0.75m_0$, and dielectric constant $\epsilon_{\mathrm{Al_2O_3}}=3.9$.

The wave functions and energies associated with the calculation of the 2DEG with a 10 Å barrier are shown in Fig. 5. As is evident in Fig. 5(a), the confining potential for the 2DEG is quite shallow and weak; the depth of the potential is only a few hundred meV and the potential does not flatten out until about 300 Å from the interface. Two subbands are occupied up to the Fermi level. The wave functions of the two subbands are shown in Fig. 5(b), and the density distribution in the 2DEG is shown in Fig. 5(c).

The numerical results for the coupling of the first subband of the InAs surface layer with a ferromagnetic gate are shown in Fig. 6, as a function of the Al_2O_3 barrier thickness. The coupling for the second subband is an order of magnitude weaker, and because only $\approx$20% of the carriers are in this subband, we neglect its presence from now on. The spin splitting is negligible except for intimate contact, in which case the value of $\approx$10 meV means a polarization of the gas of $\approx$15%. This value is quite high and is achievable in this system because the barrier is unnecessary for the creation of the 2DEG.

The scattering times for the two spin channels approach the sub-picosecond range for the thinnest barriers and intimate contact. The intrinsic scattering time of the surface InAs 2DEG is in the hundreds of femtosecond range at low temperatures, corresponding to a mobility of $\approx$ 7000 cm^2/V s.[31] The coupling has been calculated down to an oxide thickness of 1 Å; the tight-binding model breaks down for intimate contact.

IV. SPIN-DEPENDENT TRANSPORT UNDER THE FERROMAGNET

We have calculated the spin-dependent self-energy for 2DEG states coupled to a ferromagnetic gate, which in general results in (1) a spin-dependent scattering time associated with the interaction of the 2DEG electrons with the ferromagnet $\tau_{\pm}$ and (2) a spin splitting ($|\Delta_+-\Delta_-|$ in the single subband limit) resulting in unequal electron densities in the two spin channels $N_{\pm}$. In this section we examine the influence of these two results of the coupling on the in-plane

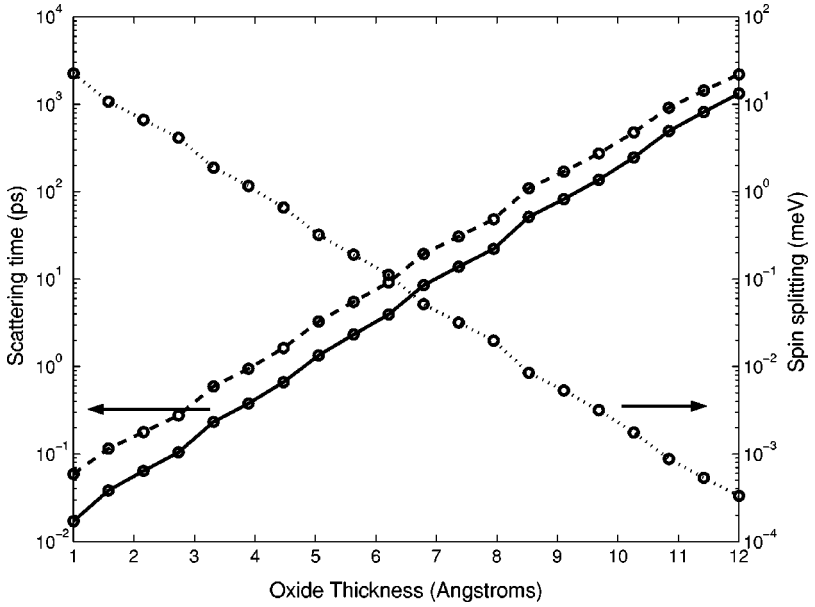

FIG. 6. A plot of the spin splitting $|\Delta_+-\Delta_-|$ (dotted line running from upper left to lower right) and the spin-dependent scattering times τ_+ (full line running from lower left to upper right) and τ_- (dashed line running from lower left to upper right) as a function of the thickness of the Al_2O_3 barrier for the lowest subband in the InAs surface layer. The parameters used are explained in the text.

transport of the 2DEG, and find that (1) the in-plane conductivity becomes spin dependent and (2) 2DEG electrons can irreversibly leak into the ferromagnetic gate in a spin-dependent manner (if the ferromagnet is biased with respect to the semiconductor).

We derive the transport equations in the 2DEG, accounting for current leakage into the gate and, therefore, the density variation along the semiconductor channel. In the following we assume that the current in the 2DEG flows in the $\hat{x}$ direction. The boundary condition on the channel density will be that at the source and drain contacts the 2DEG takes its equilibrium density related to the confinement and the Fermi energy of the 2DEG. The growth axis is in the $\hat{z}$ direction, with the ferromagnet interface at $z=0$. The electron confinement in the $\hat{z}$ direction is assumed to be constant along the channel. The system is homogeneous in the $\hat{y}$ direction, so there is no y dependence in any of the equations. The two spin channels are considered to be completely decoupled throughout the device (valid for channel lengths smaller than the spin relaxation length).

The continuity equation for 2DEG electrons is

$$\frac{\partial}{\partial t} n_{\pm}(x,z,t) + \vec{\nabla} \cdot \vec{j}_{\pm}(x,z,t) = 0, \tag{23}$$

where $n_{\pm}(x,z,t)$ is the spin-dependent particle density (cm^{-3}) and $\hat{j}_{\pm}(x,z,t)$ is the spin-dependent particle current ($\mathrm{cm}^{-2}\,\mathrm{s}^{-1}$). In the steady-state,

$$\frac{\partial}{\partial x} j_{x,\pm}(x,z) = -\frac{\partial}{\partial z} j_{z,\pm}(x,z). \tag{24}$$

Integrating out the z dependence through the semiconductor up to the interface at $z=0$ we obtain

$$\begin{aligned} \frac{\partial}{\partial x} J_{x,\pm}(x) &= -j_{z,\pm}(x,z=0) + j_{z,\pm}(x,z=-\infty) \\ &= -j_{z,\pm}(x,z=0), \end{aligned} \tag{25}$$

where $J_{x,\pm}(x) = \int_{-\infty}^{0} dz\, j_{x,\pm}(x,z)$ is the integrated 2DEG current flowing in the $\hat{x}$ direction. The term $j_{z,\pm}(x,z=0)$ represents the leakage of 2DEG electrons irreversibly into the ferromagnetic gate and will be discussed separately for the silicon and InAs systems below. The term $j_{z,\pm}(x,z=-\infty)$ represents the electrons that are injected from the semiconductor substrate into the 2DEG. This process is unfavorable because electrons are injected into the 2DEG much more efficiently from the source and drain contacts,[32] so that $j_{z\pm}(x,z=-\infty)=0$.

The Drude conductivity is ordinarily

$$\sigma_0 = \frac{N_0 e^2 \tau_0}{m^{\star}}, \tag{26}$$

where N_0 is the 2DEG density (cm^{-2}), $-e$ is the electron charge, τ_0 is the intrinsic lifetime, and $m^{\star}$ is the effective mass of the electrons. The coupling of the 2DEG with the ferromagnet introduces spin dependence to the 2DEG density N_0 and lifetime τ_0, and, hence, to the conductivity,

$$\sigma_{\pm} = \frac{N_{\pm} e^2 \tilde{\tau}_{\pm}}{m^{\star}}, \tag{27}$$

where $N_{\pm}(x) = \int_{-\infty}^{0} dz\, n_{\pm}(x,z)$. The spin-dependent lifetime $\tilde{\tau}_{\pm}$ includes both the intrinsic 2DEG lifetime τ_0 and the spin-dependent scattering time associated with the ferromagnet $\tau_{\pm}$,

$$\tilde{\tau}_{\pm} = \left(\frac{1}{\tau_0} + \frac{1}{\tau_{\pm}} \right)^{-1}. \tag{28}$$

The spin dependence in the conductivity will affect the transport of the 2DEG only if the spin-dependent densities $N_{\pm}$ are very different or the spin-dependent scattering times $\tau_{\pm}$ are very different and are comparable to the intrinsic 2DEG lifetime τ_0.

Using this conductivity, the in-plane charge current is

$$-e J_{x,\pm}(x) = \sigma_{\pm}(x) E_x + e D_{\pm}(x) \frac{\partial}{\partial x} N_{\pm}(x). \tag{29}$$

The diffusion constant $D_{\pm}(x)$ can be related to the conductivity using the Einstein relation, and at finite temperature in two dimensions is

$$D_{\pm}(x) = \frac{\epsilon_{\pm}^{\mathrm{F}}(x) \tilde{\tau}_{\pm}}{m^{\star}} \left(1 - e^{-\epsilon_{\pm}^{\mathrm{F}}(x)/k_{\mathrm{B}}T}\right)^{-1}, \tag{30}$$

where $\epsilon_{\pm}^{\mathrm{F}}(x) = \hbar^2/2m^{\star}[4\pi N_{\pm}(x)]$ is the chemical potential at $T=0$. The in-plane field E_x results from a source-drain bias and is approximately constant throughout the 2DEG (we do not consider the feedback of the 2DEG density variation on the in-plane field, i.e., by coupling them through the Poisson equation). The in-plane charge current, Eq. (29), and the current leakage, Eq. (25), are to be solved jointly to specify completely the spin-dependent density profile $N_{\pm}(x)$ along the channel. We do this separately for the two systems under consideration.

A. Silicon inversion layer

A gate bias is necessary to create the inversion layer in silicon MOSFET-style device. We assume that the normal-metal gate is replaced with a ferromagnet, so that the ferromagnet is biased with respect to the silicon substrate. The Fermi level in the ferromagnet is lower than the Fermi level in the semiconductor. Hence 2DEG electrons can tunnel into the ferromagnetic gate, inelastically fall to the Fermi level in the ferromagnet, and have no way to get back into the semiconductor. This causes a leakage of the 2DEG density, so that the current is not constant along the channel,

$$\frac{\partial}{\partial x} J_{x,\pm} = -j_{z,\pm}(x,z=0) = \frac{-N_{\pm}(x)}{\tau_{\pm}}. \tag{31}$$

Combining Eq. (31) with Eq. (29), we have the differential equation specifying the spin-dependent channel density:

$$\frac{\partial}{\partial x}\left(D_{\pm}(x)\frac{\partial N_{\pm}}{\partial x}\right)+\frac{eE_x\tilde{\tau}_{\pm}}{m^{\star}_{\mathrm{Si,t}}}\frac{\partial N_{\pm}}{\partial x}-\frac{N_{\pm}(x)}{\tau_{\pm}}=0. \quad (32)$$

The spin-dependent scattering times $\tau_{\pm}$ depend on the thickness of the oxide barrier under consideration. We have assumed that, except for at the source and drain, the system is homogeneous in x and that the lifetimes and scattering times are independent of the density variation throughout the channel.

Because the diffusion constant is dependent upon the density in a complicated way, Eq. (32) must be solved numerically. In the limit where the diffusion constant does not depend on x, the solution under a single gate is

$$N_{\pm}(x)=A_{\pm}e^{-x/l^{\mathrm{down}}_{\pm}}+B_{\pm}e^{x/l^{\mathrm{up}}_{\pm}}, \quad (33)$$

where the *downstream* and *upstream* lengths[13,14] are

$$l^{\mathrm{down}}_{\pm}=\frac{-eE_x\tau_{\pm}\tilde{\tau}_{\pm}}{2m^{\star}_{\mathrm{Si,t}}}\left(\sqrt{1+\frac{4D_{\pm}(m^{\star}_{\mathrm{Si,t}})^2}{(eE_x)^2\tau_{\pm}\tilde{\tau}^2_{\pm}}}+1\right), \quad (34)$$

$$l^{\mathrm{up}}_{\pm}=\frac{-eE_x\tau_{\pm}\tilde{\tau}_{\pm}}{2m^{\star}_{\mathrm{Si,t}}}\left(\sqrt{1+\frac{4D_{\pm}(m^{\star}_{\mathrm{Si,t}})^2}{(eE_x)^2\tau_{\pm}\tilde{\tau}^2_{\pm}}}-1\right), \quad (35)$$

and $A_{\pm}$ and $B_{\pm}$ are fixed by the boundary conditions. Note that in all calculations in this paper, the in-plane electric field E_x was taken as negative, so that $l^{\mathrm{up}}_{\pm}$ and $l^{\mathrm{down}}_{\pm}$ are defined to always be positive numbers. The real solution, which is calculated numerically with $D_{\pm}(x)$ varying along the channel, is more complicated, but the above approximation captures the qualitative aspects of the channel density. The density starts at its equilibrium value near the source and the drain, which act as reservoir's for electrons. The electrons leak into the gate, causing the density to decrease as they move further from the source or drain. In the absence of a source-drain bias, the decay of the density would be symmetric about the center of the gate; a finite source-drain bias breaks the symmetry, and hence gives the two decay lengths $l^{\mathrm{up}}_{\pm}$ and $l^{\mathrm{down}}_{\pm}$. The spin-dependent channel density $N_{\pm}(x)$ determines the spin-dependent channel current via Eq. (29).

The 2DEG density and current for the silicon inversion layer coupled to a ferromagnetic gate are shown in Fig. 7 and Fig. 8 for the low-field regime $E_x=0$ V/cm and the high-field regime $E_x=-5000$ V/cm, respectively. The source is at $x_{\mathrm{L}}=0$, the drain is at $x_{\mathrm{R}}=1000$ Å, and both spin channels take their equilibrium density at the source and drain, $N_{\pm}(x_{\mathrm{L}})=N_{\pm}(x_{\mathrm{R}})=0.5\times10^{12}$ cm^{-2}. The oxide is assumed to be 6 Å thick, so that the spin-dependent scattering times are $\tau_{+}=3$ ps and $\tau_{-}=6$ ps. The intrinsic scattering time is taken as 1 ps, and the temperature is 10 K. The spin-dependent density and current were calculated by solving the linear system of equations that results from the finite differencing of the differential equation specifying the density [Eq. (32)]. The solution was iterated until both the density $N_{\pm}(x)$ and the diffusion constant $D_{\pm}(x)$ converged. This method was used to calculate the current and density for the remainder of the paper.

The effects of the leakage of channel carriers are immediately evident in Fig. 7. Carriers under the gate can irreversibly leak into the gate. A diffusion current flows from the source and from the drain into the 2DEG to replace the leaking electrons. The channel density is symmetric about the center of the device, and the current flows in opposite directions on the two sides of the gate. The spin dependence due to the different scattering times for the two spin channels is evident; the + channel, which leaks at a faster rate, falls to a lower density in the center of the gate, and has higher currents near the source and drain due to the larger gradient in the density as compared to the − channel.

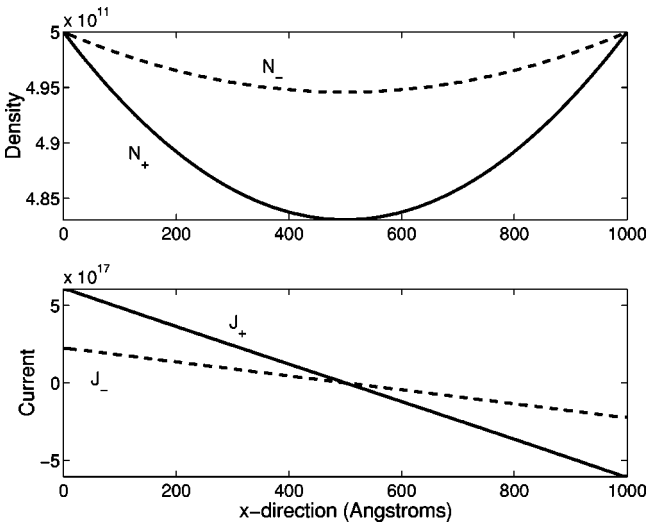

FIG. 7. The spin-dependent 2DEG density (cm^{-2}) and spin-dependent 2DEG current (cm^{-1} s^{-1}) under a single ferromagnetic gate for the silicon inversion layer for *zero* source-drain bias (in-plane field of $E_x=0$ V/cm). There is a diffusion current flowing from both the source and the drain into the gate. The other parameters used are explained in the text.

As the field is turned up, the drift term in Eq. (29) fights against the backflow at the drain contact. At

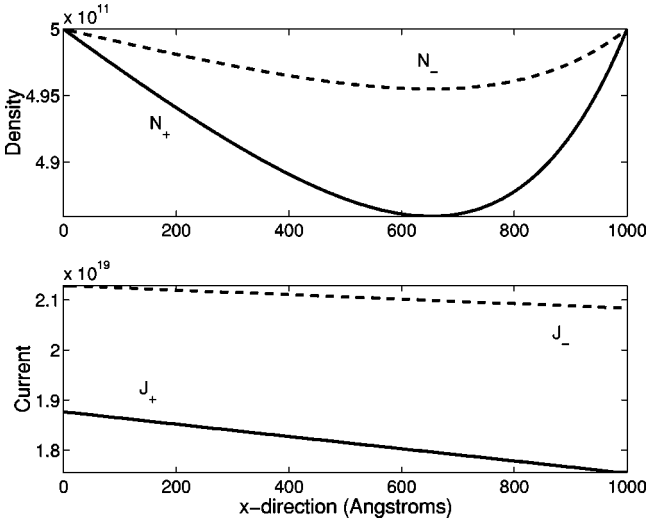

FIG. 8. The spin-dependent 2DEG density (cm^{-2}) and spin-dependent 2DEG current (cm^{-1} s^{-1}) under a single ferromagnetic gate for the silicon inversion layer for an extremely high in-plane field of $E_x=-5000$ V/cm. The other parameters used are explained in the text.

≈ -200 V/cm, the drift current overcomes the diffusive backflow and the current through the drain becomes positive. Curiously, the field at which the drift current cancels the diffusion current is spin dependent, so that it is possible to create the following situations: (1) the drift current cancels the diffusion current for one of the spin channels, but not the other, so that the net current that flows through the drain is 100% spin polarized, and (2) the current for one spin channel is positive while the current in the other spin channel is exactly opposite, so that no net current flows out of the drain, but a *pure* spin current flows out the drain. Further study of the pure spin current in the single ferromagnetic gate silicon system will be given in a future publication.

In Fig. 8, a very high in-plane field is strong enough to overcome the backflow from the drain; the asymmetry induced by the strong source-drain bias is evident in the plot of the spin-dependent density. The transport is dominated by the drift term in Eq. (29) due to the high in-plane field; the diffusion current is only a small correction. More current is carried in the $-$ spin channel than the $+$ spin channel because the lifetime for the $-$ spins, $\tilde{\tau}_-$, is longer than the lifetime for the $+$ spins, $\tilde{\tau}_+$.

B. InAs surface layer

The 2DEG at the surface of InAs is natural and hence no gate bias on the ferromagnet is necessary. This keeps the Fermi levels in the semiconductor and in the ferromagnet equal; no electrons will leak into the gate. The in-plane current in each spin channel must be conserved,

$$\frac{\partial}{\partial x} J_{x,\pm} = 0. \tag{36}$$

The equation specifying the channel density is, from Eqs. (29) and (36),

$$\frac{\partial}{\partial x}\left(D_{\pm}(x) \frac{\partial N_{\pm}}{\partial x} \right) + \frac{eE_x \tilde{\tau}_{\pm}}{m^{\star}_{\mathrm{InAs}}} \frac{\partial N_{\pm}}{\partial x} = 0. \tag{37}$$

The spin-dependent density in the limit of $D_{\pm}(x) =$ constant is

$$N_{\pm}(x) = A_{\pm} + B_{\pm} e^{x/d_{\pm}}, \tag{38}$$

with $A_{\pm}$ and $B_{\pm}$ specified by the boundary conditions and the decay length $d_{\pm} = m^{\star}_{\mathrm{InAs}} D_{\pm} / (-eE_x \tilde{\tau}_{\pm})$. The decay lengths are similar to the expressions found in Refs. 13 and 14 for infinite spin lifetime. Because of the spatial dependence of the diffusion constant, the real solution is more complicated, but the qualitative results still hold.

The in-plane field drives a spin accumulation at one of the boundaries. A boundary condition which specifies that the density is the same at the source and drain would prevent this from happening, resulting in a constant density throughout the channel. The diffusion term in Eq. (29) vanishes, so that the current is only given by the drift term. The current carried by each spin channel must be constant due to the absence of any 2DEG leakage. For zero source-drain bias, the current is thus zero in both spin channels. This is in marked contrast with the results for the silicon case, Fig. 7, in which a diffusion current flowed towards the center of the gate from both the source and the drain at zero source-drain bias. This simple behavior of the InAs surface layer with a single ferromagnetic gate is radically altered when two gates replace the single gate, as explained below.

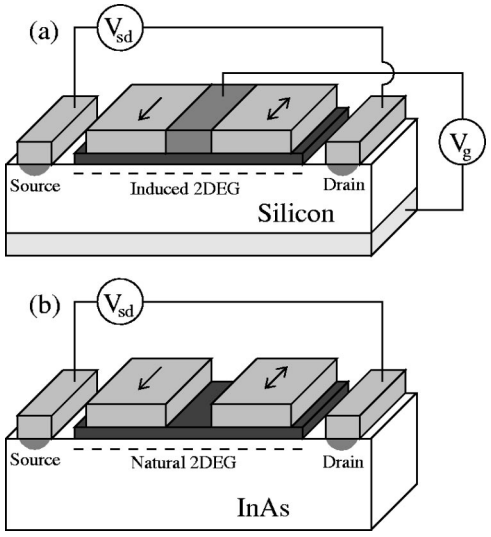

FIG. 9. Schematic diagrams of the spin-valve proposal in (a) the silicon and (b) the InAs systems. The device consists of normal nonmagnetic source and drain contacts and two ferromagnetic gates. A source drain bias V_{sd} creates the in-plane field E_x. In (a), a gate voltage V_{g} is necessary to induce the inversion in the silicon system. The space between the ferromagnets is filled with a nonmagnetic metal. In (b), no gate voltage is necessary in the InAs system. An ultrathin oxide separates the ferromagnetic gates from the 2DEG in both systems, although the oxide can be omitted in (b).

V. SPIN VALVE WITH TWO ADJACENT FERROMAGNETIC GATES

Because of the general spin dependence in the 2DEG density and current as shown above, we now discuss a simple spin-valve-type device to test the spin effects predicted by the theory. The spin effects could not be seen in transport experiments with a single gate and nonmagnetic source and drain contacts. This is because the two spin channels are measured in parallel; switching the gate magnetization would exchange the roles of the two spin channels but would have no effect on the total current measured. The single-gate spin effects could in principle be measured through other spin-dependent means, but we concentrate here on transport effects that would be more useful in device considerations.

To see the spin effects in transport experiments, we proposed a simple spin-valve design[12] shown in Fig. 9. The single gate in a normal MOSFET-style device is replaced by two ferromagnetic gates that are very near to each other. If a gate bias is applied (such as in the silicon system), the space between the two ferromagnets can be filled with a nonmagnetic metal such as aluminum in order to ensure that the 2DEG confinement is uniform between the source and the drain. The nonmagnetic metal between the two ferromagnets is not necessary in systems with no gate bias (such as the InAs system). There is some anisotropy in the design of the

two ferromagnets (either through geometry or material) so that the two ferromagnets have different coercive fields, which allows the switching of the magnetization of the second ferromagnet while leaving the magnetization of the first unchanged. Because the two spin channels are effectively decoupled throughout the device (due to the long spin-flip time), the addition of the second ferromagnet has a profound influence on the total current that flows in the 2DEG. This is because both the density and the current in each spin channel must be continuous throughout the device. This matching depends on the relative orientation of the magnetizations. The net effect is that the total current measured through the device will depend on the relative orientation of the magnetization of the two ferromagnets, which is a magnetoresistance effect. The first ferromagnet will be referred to as the first ''gate,'' and the second ferromagnet will be referred to as the second gate.

Although we propose such a device as a way to test the predictions of the theory, the device as is could do perform the role of a memory element. The magnetization of the first gate remains fixed, while the orientation of the second gate's magnetization depends on whether the information you are trying to read out is a ''0'' or a ''1.'' The measurement of the second gate's magnetization is read out by measuring the current at the drain contact. The bit could be written using a local magnetic field (created by nearby wires, as in current MRAM technology) that is strong enough to switch the second gate without switching the first gate. The two main benefits of such a design are that (1) the nonvolatile information storage has been incorporated onto the semiconductor, where the information processing occurs, and (2) we take advantage of the necessity for ultrathin oxide barriers due to the aggressive scaling of MOSFET technology to the nanometer scale (whereas currently the ability of 2DEG carriers to interact with the gate through an ultrathin oxide barrier is seen as a major obstacle to be avoided). Once demonstrated, other device designs can be explored which do not rely on analogy to existing structures to fully benefit from the new spin effects.

Below we discuss the spin valve for the silicon and InAs systems separately. To model the 2DEG density and current throughout the spin-valve, we assume the following. The source is at $x_L=0$ and the drain is at $x_R=2200$ Å. Both gates are 1000 Å wide and the gap between the two gates is 200 Å, so that the left side of the gap is at $x_A=1000$ Å and the right side of the gap is at $x_B=1200$ Å.

The spin-dependent density with parallel gate magnetization is $N_{\pm}^{p}(x)$, where $\pm$ refers to the electron's spin under with respect to the first gate and p refers to parallel. The density and current must be continuous throughout the device. The spin-dependent scattering times are no longer constant along the channel due to the addition of the second gate, so that for parallel gate magnetizations,

$$\tau_{\pm}^{p}(x)=\begin{cases}\tau_{\pm}, & x_L<x<x_A\\ \infty, & x_A<x<x_B\\ \tau_{\pm}, & x_B<x<x_R,\end{cases} \tag{39}$$

and the spin-dependent lifetimes are

$$\tilde{\tau}_{\pm}^{p}(x)=\begin{cases}\tilde{\tau}_{\pm}, & x_L<x<x_A\\ \tau_0, & x_A<x<x_B\\ \tilde{\tau}_{\pm}, & x_B<x<x_R.\end{cases} \tag{40}$$

$\tilde{\tau}_{\pm}$ is specified by Eq. (28). The density and current in both the silicon and InAs systems can now be calculated for parallel magnetization.

For antiparallel gate magnetizations, the second gate magnetization is flipped with respect to that of the first gate, so the spin-dependent scattering times for antiparallel gate configuration are

$$\tau_{\pm}^{ap}(x)=\begin{cases}\tau_{\pm}, & x_L<x<x_A\\ \infty, & x_A<x<x_B\\ \tau_{\mp}, & x_B<x<x_R,\end{cases} \tag{41}$$

and the spin-dependent lifetimes are

$$\tilde{\tau}_{\pm}^{ap}(x)=\begin{cases}\tilde{\tau}_{\pm}, & x_L<x<x_A\\ \tau_0, & x_A<x<x_B\\ \tilde{\tau}_{\mp}, & x_B<x<x_R.\end{cases} \tag{42}$$

The obvious difference from the parallel case is the exchange of the roles of spins $+$ and $-$ under the second gate ($\tau_{\pm}\rightarrow\tau_{\mp}$ and $\tilde{\tau}_{\pm}\rightarrow\tilde{\tau}_{\mp}$).

For both parallel and antiparallel gate magnetizations the density for both spin channels must take on its equilibrium value at the source and drain, which we assume for both the silicon and InAs systems is 0.5×10^{12} cm^{-2} for each spin channel, so that the boundary conditions are

$$\left.\begin{matrix}N_{\pm}^{p}(x_L)\\ N_{\pm}^{p}(x_R)\\ N_{\pm}^{ap}(x_L)\\ N_{\pm}^{ap}(x_R)\end{matrix}\right\}=0.5\times10^{12}\ \text{cm}^{-2}. \tag{43}$$

These boundary conditions are sufficient to fully calculate the spin-dependent density and current throughout the spin valve for parallel and antiparallel gate magnetizations. These are used next to calculate the density and current in the two-gate spin-valve proposal for the silicon and InAs systems separately.

A. Silicon inversion layer

A schematic diagram of the silicon spin valve is shown in Fig. 9(a). The addition of the second gate causes the scattering times and lifetimes to become dependent upon x. For parallel gate magnetizations, the differential equation that must be solved is

$$\frac{\partial}{\partial x}\left(D_{\pm}^{p}\frac{\partial N_{\pm}^{p}}{\partial x}\right)+\frac{eE_x}{m_{\text{Si,t}}^{\star}}\frac{\partial}{\partial x}(\tilde{\tau}_{\pm}^{p}N_{\pm}^{p})-\frac{N_{\pm}^{p}}{\tau_{\pm}^{p}}=0. \tag{44}$$

where the spin-dependent scattering time and lifetime along the channel are specified by Eq. (39) and Eq. (40), respectively. These equations must be solved numerically as previously described, with the boundary conditions, Eq. (43).

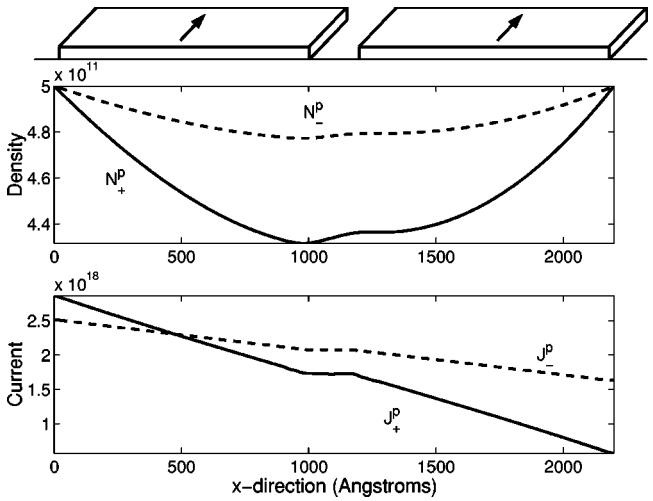

FIG. 10. The density (cm^{-2}) and current ($cm^{-1}\,s^{-1}$) for a silicon inversion layer with parallel gate magnetizations. The parameters are explained in the text.

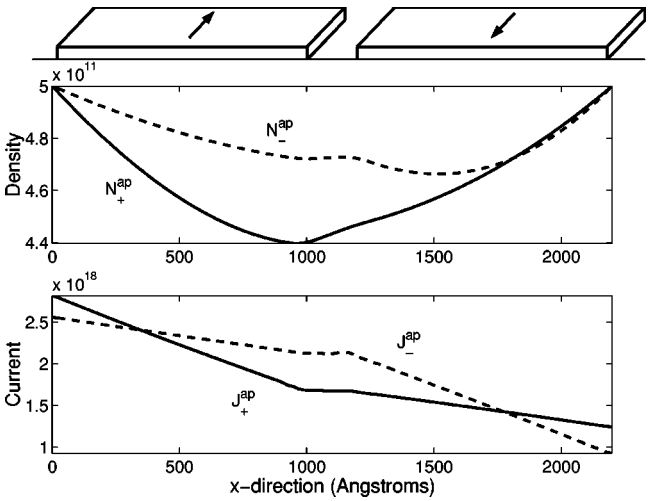

FIG. 11. The density (cm^{-2}) and current ($cm^{-1}\,s^{-1}$) for a silicon inversion layer with antiparallel gate magnetizations. The two spin channels are labeled with respect to the first gate.

The density and current in the silicon inversion layer with parallel gate magnetization are shown in Fig. 10. The in-plane field that drives the current is $E_x=-500$ V/cm and the temperature is 10 K. The intrinsic scattering time is $\tau_0=1$ ps and the spin-dependent scattering times are $\tau_+=3$ ps and $\tau_-=6$ ps, consistent with a 6 Å barrier. The behavior is very different compared to the single gate case, Fig. 8. The conductivity changes from under the first gate to the gap region (likewise from the gap region to under the second gate). Because E_x is constant, this requires that the density adjusts itself to make both the density and current continuous. Spin accumulation can result if the in-plane driving field is sufficiently strong. Note that the current in the gap region of the device is constant because there is no electron leakage in this region.

For antiparallel gate magnetizations, the differential equation that must be solved is the same as for the parallel case [Eq. (44)], except change $p\rightarrow ap$ in all superscripts. The scattering time is specified by Eq. (41) and the lifetime is specified by Eq. (42). Compared to the device with parallel magnetization, we see marked differences in both the density and current in the antiparallel case (see Fig. 11). Again, this is because when crossing through the different regions of the device, the density and current must be continuous. Compared to the parallel case, the $+$ spin channel now sees the conductivity and leakage of the $-$ spin channel under the second gate, so the matching is completely different. The total current is different in the two cases, causing a magnetoresistance effect.

To clearly see the magnetoresistance effect caused by the switching of the second gate's magnetization, in Fig. 12 we plot the following magnetoresistance percentage:

$$\mathrm{MR}=100\left|\frac{J_x^{\mathrm{p}}(x_{\mathrm{R}})-J_x^{\mathrm{ap}}(x_{\mathrm{R}})}{J_x^{\mathrm{p}}(x_{\mathrm{R}})}\right|, \tag{45}$$

where $J_x^{\mathrm{p}}(x_{\mathrm{R}})$ and $J_x^{\mathrm{ap}}(x_{\mathrm{R}})$ are the sum of the current in the two spin channels with parallel magnetization and antiparallel magnetization, respectively. The current is assumed to be measured at the drain ($x=x_{\mathrm{R}}$). All parameters are the same as previously discussed. The magnetoresistance is quite small for large in-plane driving fields, where the drift current dominates the transport. The difference between the parallel and antiparallel currents, $J_x^{\mathrm{p}}(x_{\mathrm{R}})-J_x^{\mathrm{ap}}(x_{\mathrm{R}})$, is small compared to $J_x^{\mathrm{p}}(x_{\mathrm{R}})$ [or $J_x^{\mathrm{ap}}(x_{\mathrm{R}})$] because of the strong drift. As the in-plane field is decreased, the diffusion current becomes more important, which opposes the drift current at the drain. The different density profiles in the parallel and antiparallel cases imply that the diffusion current a the drain contact is different in the two cases; the spin effects are more pronounced and the magnetoresistance grows. At some critical field (≈ -200 V/cm) the drain current for parallel magneti-

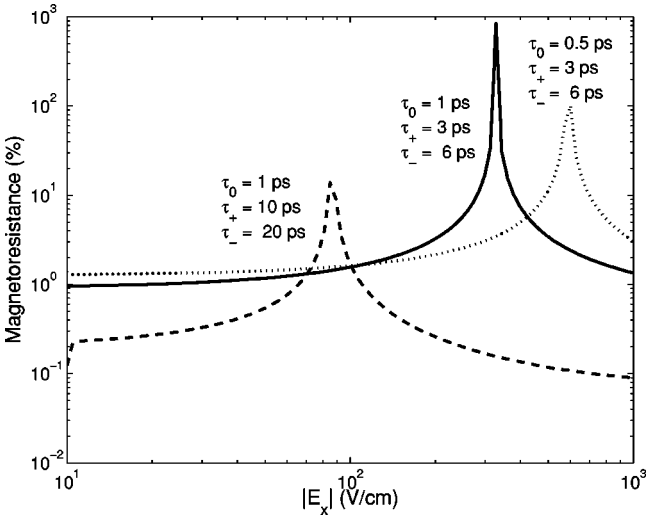

FIG. 12. The full line is the magnetoresistance [Eq. (45)] as a function of the in-plane driving field E_x, using the same parameters as in Figs. 10 and 11. The dashed line is the magnetoresistance using scattering times appropriate for a thicker barrier. The dotted line is the magnetoresistance for a shorter intrinsic scattering time. The high-field limit of this plot was discussed in Ref. 12.

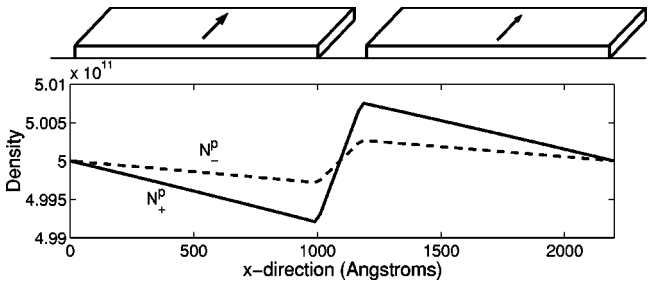

FIG. 13. The density (in units of cm^{-2}) for an InAs surface layer with parallel gate magnetizations. The parameters are explained in the text.

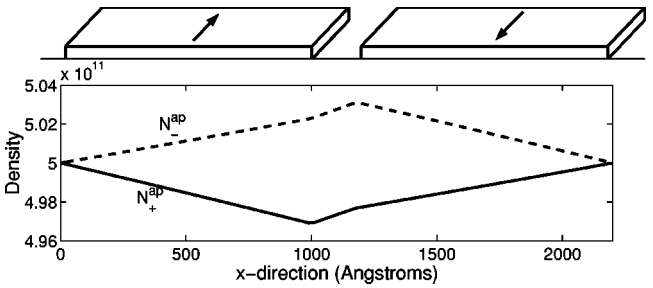

FIG. 14. The density (cm^{-2}) for an InAs surface layer with antiparallel gate magnetization. The two spin channels are labeled with respect to the first gate. The parameters are explained in the text.

zations equals zero; the drift current flowing in the $+\hat{x}$ direction is exactly canceled by the diffusion current flowing in the $-\hat{x}$ direction. Due to the way in which Eq. (45) is defined, this causes a divergence of the magnetoresistance. As the in-plane field is reduced further, the total current in the parallel configuration becomes negative as the diffusive backflow overtakes the drift current at the drain. At low source-drain bias the drain current in both the parallel and antiparallel configurations is negative as the backflow completely dominates the current; a small magnetoresistance is still present. The spin valve would ideally be operated just above the critical field, where the drain current is still positive but the effects of the diffusion current are important.

In addition, the dashed line in Fig. 12 is the same calculation using the scattering times for a thicker oxide barrier. The effect is still present but moves to a lower in-plane field. This is because there is less leakage, and hence the diffusive backflow at the drain is lower than for a thinner barrier. The dotted line in Fig. 12 is the calculation using a shorter intrinsic scattering time, which has the effect of moving the magneoresistance peak to a higher in-plane field. Shortening the intrinsic scattering time decreases the conductivity, and hence a higher field is necessary to balance the drift and diffusion currents.

B. InAs surface layer

A schematic diagram of the InAs system is shown in Fig. 9(b). For parallel magnetizations, the differential equation that must be solved is

$$\frac{\partial}{\partial x}\left(D^{\mathrm{p}}_{\pm}\frac{\partial N^{\mathrm{p}}_{\pm}}{\partial x}\right)+\frac{eE_x}{m^{\star}_{\mathrm{InAs}}}\frac{\partial}{\partial x}(\tilde{\tau}^{\mathrm{p}}_{\pm}N^{\mathrm{p}}_{\pm})=0, \tag{46}$$

where the scattering times and lifetimes are specified by Eq. (39) and Eq. (40) and the boundary conditions are specified by Eq. (43).

The density in the InAs surface layer with parallel gate magnetization are shown in Fig. 13. The in-plane field that drives the current and the boundary conditions on the source and drain densities are the same as in the silicon case discussed previously. The intrinsic scattering time is taken as 0.1 ps, and the spin-dependent scattering times are taken as $\tau_+=0.3$ ps and $\tau_-=1$ ps, consistent with a barrier of less than 5 Å. In contrast to the single gate case, the density is not constant throughout the device, because it must adjust itself at the interfaces between the three regions to keep the current constant. Both spin channels must decrease their density in the gap region to keep the current constant, but the density profile for the two spin channels is very different because the lifetimes are different in the gate regions. This process leads to a static spin polarization at the interfaces between different regions of the device, or spin accumulation. This accumulation must decay back to the equilibrium value at the drain. The current in each spin channel is constant throughout the device (1.47×10^{18} cm^{-1} s^{-1} for the + channel, 1.74×10^{18} cm^{-1} s^{-1} for the − channel) due to the ''floating'' gates.

For the thinnest of oxides and intimate contact, Fig. 6 implies that the spin splitting becomes important. This would make the equilibrium values for the two spin channels at the source and drain spin dependent. This asymmetry further enhances the spin effects due just to the scattering time; the qualitative picture remains the same.

For antiparallel gate magnetizations, the differential equation is the same as for the parallel case [Eq. (46)], except change $p\rightarrow ap$ in all superscripts. The scattering times and lifetimes are given by Eqs. (41) and (42). As has already been discussed, the density and current are quite different from the parallel case due to different matching conditions for each of the spin channels. The density is plotted in Fig. 14. Because of the exchanging of the roles of the two spin channels under the second gate, the density for the + channel increases to well over its equilibrium value in the gap region, and the − channel decreases to well below its equilibrium value. Again, this is another example of spin accumulation at the interfaces between different regions of the device. The current in each spin channel is constant throughout the device ($\approx1.6\times10^{18}$ $\mathrm{cm}^{-1}\,\mathrm{s}^{-1}$ for both spin channels).

The magnetoresistance, Eq. (45), is relatively constant at $\approx1\%$ for all reasonable in-plane fields. This is because the diffusion term is always much smaller than the drift term (the spin accumulation that occurs is always very small, much smaller than the leakage-induced changes in the density in the silicon system), so that the magnetoresistance is basically just specified by the difference in the spin-dependent lifetimes. There is never any backflow, as in the silicon case, so the divergent structure in the silicon magnetoresistance (see

Fig. 12) is not seen in the InAs case. Because the coupling between the InAs surface electron layer and the ferromagnetic gate is so strong, the spin-flip time does not have a significant effect upon the value of the magnetoresistance ratio; a spin-flip time of 1 ps only decreases the magnetoresistance ratio by a factor of 2. For thicker gate oxides (greater than ≈ 10 Å), the spin-flip time will have a much greater impact and can reduce the magnetoresistance ratio by a factor 100 or more.

VI. CONCLUSIONS

We presented above a comprehensive theoretical treatment of the spin-dependent electronic and transport properties of a two-dimensional electron gas, under the strong influence of the proximity of a ferromagnetic layer. By constructing an appropriate Green's function, we determined the complex self-energy of the quantum confined electrons in the semiconductor, which are coupled quantum mechanically with the spin-polarized Fermi sea in the ferromagnet. Using a tight-binding-like Hamiltonian that couples the two regions, we calculated the spin-dependent properties of two paradigmatic systems: (i) the gate-induced inversion layer in a ferromagnetic metal-oxide-silicon junction; and (ii) the (spontaneous) accumulation layer of InAs separated from a ferromagnet by a thin oxide barrier. The ferromagnetic proximity induces a spin splitting of the quantum confined subbands in the semiconductor and a spin-dependent broadening, which make the in-plane transport spin dependent. We studied extensively the dependence of the ferromagnetic proximity as a function of the thickness of the thin oxide layer separating the semiconductor from the metal. Our results show that the spin-dependent lifetime broadening is the main effect, whereas the spin splitting becomes sizeable only for nearly intimate contact between the semiconductor and the ferromagnet.

Knowledge of the spin-dependent electronic properties of the two-dimensional electron gas led to a treatment of the in-plane transport of spin-dependent current. The leakage current into the gate creates a density gradient along the semiconducting layer. The resultant drift and diffusion terms of the source to drain current in the semiconductor were treated above in a self-consistent manner with the leakage and the density variation. While the leakage current is usually considered a limitation for electronic field-effect transistors with very thin oxide layers, the leakage current plays a positive role in the spin dependence of the transport. We applied our transport theory to our recently proposed spin valve with two neighboring ferromagnetic gates. The detailed results of the spin-dependent steady-state densities and currents for different configurations of the magnetization in the gates yielded an explicit understanding of dependence of the magnetoresistance as a function of the source-drain bias. Notably, for a critical bias, a pure spin current (i.e., with a zero net charge current) can be created at the drain contact. This effect is caused by the gate leakage (e.g., for the silicon inversion layer) and is due to the compensation of net drift and diffusion currents.

We hope that the interesting new physics in the transport governed by the proximity effect will stimulate further explorations by experiments and by more realistic simulations, opening up the possibility of creating field-effect spintronics devices as an alternative to spin injection devices.

ACKNOWLEDGMENTS

This work was supported by DARPA/ONR under Grant No. N0014-99-1-1096, NSF under Grant No. DMR-0099572, the Swiss National Foundation (for partial support of C.C.), and University of California Campus-Laboratories Cooperation project (for J.P.M.). We thank Edward T. Yu for helpful discussions.

[1] S.A. Wolf, D.D. Awschalom, R.A. Buhrman, J.M. Daughton, S. von Molnar, M.L. Roukes, A.Y. Chtchelkanova, and D.M. Treger, Science **294**, 1488 (2001).
[2] S. Datta and B. Das, Appl. Phys. Lett. **56**, 665 (1990).
[3] Y.A. Bychkov and E.I. Rashba, Sov. Phys. JETP **39**, 78 (1984).
[4] R. Fiederling, M. Keim, G. Reuscher, W. Ossau, G. Schmidt, A. Waag, and L.W. Molenkamp, Nature (London) **402**, 787 (1999).
[5] Y. Ohno, D.K. Young, B. Beschoten, F. Matsukura, H. Ohno, and D.D. Awschalom, Nature (London) **402**, 790 (1999).
[6] H.J. Zhu, M. Ramsteiner, H. Kostial, M. Wassermeier, H.-P. Schonherr, and K.H. Ploog, Phys. Rev. Lett. **87**, 016601 (2001).
[7] A.T. Hanbicki, B.T. Jonker, G. Itskos, G. Kioseoglou, and A. Petrou, Appl. Phys. Lett. **80**, 1240 (2002).
[8] J. Nitta, T. Akazaki, H. Takayanagi, and T. Enoki, Phys. Rev. Lett. **78**, 1335 (1997).
[9] T. Koga, J. Nitta, T. Akazaki, and H. Takayanagi, Phys. Rev. Lett. **89**, 046801 (2002).
[10] D.M. Zumbuhl, J.B. Miller, C.M. Marcus, K. Campman, and A.C. Gossard, Phys. Rev. Lett. **89**, 276803 (2002).
[11] J.B. Miller, D.M. Zumbuhl, C.M. Marcus, Y.B. Lyanda-Geller, D. Goldhaber-Gordon, K. Campman, and A.C. Gossard, Phys. Rev. Lett. **90**, 076807 (2003).
[12] C. Ciuti, J.P. McGuire, and L.J. Sham, Appl. Phys. Lett. **81**, 4781 (2002).
[13] Z.G. Yu and M.E. Flatte, Phys. Rev. B **66**, 201202 (2002).
[14] Z.G. Yu and M.E. Flatte, Phys. Rev. B **66**, 235302 (2002).
[15] R.K. Kawakami, Y. Kato, M. Hanson, I. Malajovich, J.M. Stephens, E. Johnston-Halperin, G. Salis, A.C. Gossard, and D.D. Awschalom, Science **294**, 131 (2001).
[16] R.J. Epstein, I. Malajovich, R.K. Kawakami, Y. Chye, M. Hanson, P.M. Petroff, A.C. Gossard, and D.D. Awschalom, Phys. Rev. B **65**, 121202 (2002).
[17] R.J. Epstein, J. Stephens, M. Hanson, Y. Chye, A.C. Gossard, P.M. Petroff, and D.D. Awschalom, Phys. Rev. B **68**, 041305 (2003).
[18] C. Ciuti, J.P. McGuire, and L.J. Sham, Phys. Rev. Lett. **89**, 156601 (2002).
[19] An up-to-date review is given by J.J. Akerman, I. Guedes, C.

Leighton, M. Grimsditch, and I.K. Schuller, Phys. Rev. B **65**, 104432 (2002).
[20] J.C. Slonczewski, Phys. Rev. B **39**, 6995 (1989).
[21] S.H. Lo, D.A. Buchanan, Y. Taur, and W. Wang, IEEE Electron Device Lett. **18**, 209 (1997).
[22] W.K. Shih, E.X. Wang, S. Jallepalli, F. Leon, C.M. Maziar, and A.F. Taschjr, Solid-State Electron. **42**, 997 (1998).
[23] J.M. Kikkawa, I.P. Smorchkova, N. Samarth, and D.D. Awschalom, Science **277**, 1284 (1997).
[24] J.M. Kikkawa and D.D. Awschalom, Phys. Rev. Lett. **80**, 4313 (1998).
[25] J.M. Kikkawa and D.D. Awschalom, Nature (London) **397**, 139 (1999).
[26] I. Malajovich, J.M. Kikkawa, D.D. Awschalom, J.J. Berry, and N. Samarth, Phys. Rev. Lett. **84**, 1015 (2000).
[27] T. Ando, A.B. Fowler, and F. Stern, Rev. Mod. Phys. **54**, 437 (1982).
[28] J. Hong and D.L. Mills, Phys. Rev. B **62**, 5589 (2000).
[29] B. Brar, G.D. Wilk, and A.C. Seabaugh, Appl. Phys. Lett. **69**, 2728 (1996).
[30] W.H. Rippard, A.C. Perrella, F.J. Albert, and R.A. Buhrman, Phys. Rev. Lett. **88**, 046805 (2002).
[31] S.P. Watkins, C.A. Tran, R. Ares, and G. Soerensen, Appl. Phys. Lett. **66**, 882 (1994).
[32] H.S. Momose, M. Ono, T. Yoshitomi, T. Ohguro, S.-I. Nakamura, M. Saito, and H. Iwai, IEEE Trans. Electron Devices **43**, 1233 (1996).